International Conference on Applied Energy 2019
Aug 12-15, 2019, Västerås, Sweden
Paper ID: 972

COMPARISON OF THE COOLING AND POWER SYSTEMS INTEGRATING ORC WITH CHEMISORPTION CYCLES

Ke Tang [1,2], Yiji Lu [1,2]*, Zhi Li [1], Yaodong Wang [2], Anthony Paul Roskilly [1,2], Xiaoli Yu [1,2]

1 Department of Energy Engineering, Zhejiang University, Hangzhou 310027, China
2 Sir Joseph Swan Centre for Energy Research, Newcastle University, Newcastle NE1 7RU, UK

*Corresponding author Email: luyiji0620@gmail.com (Y. Lu)

ABSTRACT

This paper conducts and compares the computational modelling of two cooling and power systems, integrating organic Rankine cycle (ORC) with adsorption cycles. The kinetic sorption models of $MnCl_2$-EG and $MnCl_2$-EG-Ni@C are established and validated via the data in previous study. The result shows a higher thermal efficiency of utilizing adsorption units as the top user of the heat source. Moreover, it is demonstrated that using the novel sorbents with Ni@C could improve the cooling production and the thermal efficiency of the cogeneration system.

Keywords: cogeneration systems, $MnCl_2$-EG-Ni@C, ORC, chemisorption

1. INTRODUCTION

The mining, transportation, utilization and storage of the conventional fuels cause severe problems such as environmental depletion. The replacement by Low-grade thermal energies, such as terrestrial heat and industrial waste heat, could be the solution.

Organic Rankine cycle (ORC) is a representative technology to convert low-grade heat into mechanical power, while chemisorption cycles could produce the refrigeration by using low thermal energy. L. Talluri et al. developed a design procedure for ORC applications, declaring 64% total-to-static efficiency [1]. S. Fujii et al. designed a thermochemical energy storage and transport system which recovered the waste heat from a sugar mill and decreased the energy consumption of 29.6 % [2]. Y. Lu et al. improved the coefficient of performance (COP) of the novel resorption system up to 38 %, by a heat and mass recovery process [3]. Some explorations were inspired to integrate these two components and realize the cogeneration systems. One of the example was the waste heat recovery system for a diesel engine designed by Y. Lu et al., indicating the enhancement of overall energy efficiency from 40 % to 47 % [4]. A dual-source chemisorption power generation system was investigated using a scroll expander, and the overall thermal efficiency achieved around 10 % [5]. F. Al-Mousawi et al. used a small-scale radial inflow turbine combining with adsorption units and achieved the power output of 785 W and the efficiency of 82 % [6]. H. Bao et al. investigated a low-grade heat driven power generation system and compared it with pumpless ORC [7]. The result showed the system was superior on energy density.

In this paper, ORC is integrated with adsorption or resorption cycles to produce cooling and power at the same time. MATLAB and REFPROP are used in the coding process. The working fluid of ORC is R245fa and the composite sorbents are Manganese chloride-expanded graphite ($MnCl_2$-EG) with or without carbon coated Nickel (Ni@C) ammonia. The refrigerant is ammonia. The kinetic models of the sorbents mentioned above are validated by the data of previous experimental works. Performance indicators include the refrigeration and thermal efficiency.

Selection and peer-review under responsibility of the scientific committee of the 11th Int. Conf. on Applied Energy (ICAE2019).

2. METHEDOLOGIES

2.1 Configurations of cogeneration systems

Four systems are built as shown in Fig 1. ORC-AD utilizes ORC as the top cycle to use the heat source from engine emission at 200 °C. Two adsorption cycles using $MnCl_2$-EG are set as the bottom cycles to use the rest of the heat source. AD-ORC substitutes the top user of LGH with adsorption cycle to compare the impact of different cycle orders R245fa is the working fluid in ORC and ammonia is the refrigerant in sorption cycles.

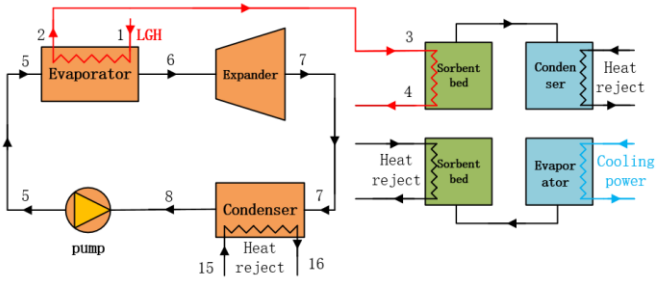

(a) ORC-AD

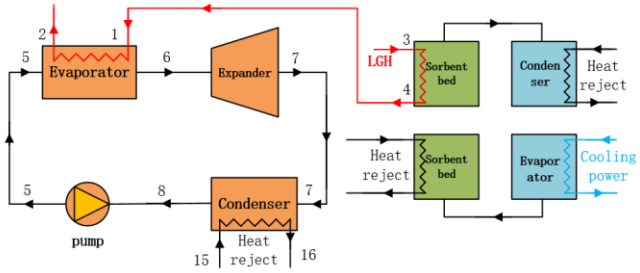

(b) AD-ORC

Fig 1 Schematic diragram of cogeneration systems

2.2 Thermodynamic analysis

The thermodynamic analysis includes the enthalpy change in the pump, evaporator, and the expander, as expresses in Equation (1) to (7). $\dot{m}_w$is the mass flow rate of the working fluid, given at 0.2 kg/s, and $\dot{m}_h$ is that of the heat source, given at 1 kg/s. Symbol h is the enthalpy with the subscripts of numbers representing for the position marked in Fig 1. H_{5s} and H_{7s} stand for the ideal enthalpy after the isentropic compression and expansion, respectively. η_i and η_m are the isentropic efficiency and the mechanical efficiency corresponding to the pump or the expander. The terms $\dot{W}_{pump}$, $\dot{W}_e$, and $\dot{W}_{net}$ are the energy caused by pump, produced by expander, and the net power generated by ORC per second, separately.

$$(h_5 - h_8) \cdot \eta_{i,pump} = h_{5s} - h_8 \quad (1)$$

$$\dot{W}_{pump} \cdot \eta_{m,pump} = \dot{m}_w \cdot (h_5 - h_8) \quad (2)$$

$$\dot{m}_w \cdot (h_6 - h_5) = \dot{m}_h \cdot (h_1 - h_2) \cdot \eta_{evap} \quad (3)$$

$$\dot{Q}_{in,ORC} = \dot{m}_w \cdot (h_6 - h_5) \quad (4)$$

$$h_6 - h_7 = (h_6 - h_{7s}) \cdot \eta_{i,exp} \quad (5)$$

$$\dot{W}_e = \dot{m}_w \cdot (h_6 - h_7) \cdot \eta_{m,exp} \quad (6)$$

$$\dot{W}_{net} = \dot{W}_e - \dot{W}_{pump} - \dot{W}_{ORC} \quad (7)$$

Equation (8) denotes the refrigeration yielded by adsorption units per unit time. Terms n_x, ΔH_r and t represent the molecular number of reacted ammonia, enthalpy change per mol ammonia and the reaction time of adsorption/desorption.

$$\dot{Q}_{ref} = n_x \cdot \Delta H_r / t \quad (8)$$

2.3 Kinetic models of adsorption and desorption

Equation (9) and (10) present the kinetic models of adsorption and desorption to obtain the ammonia conversion ratio x, respectively. A_r is the Arrhenius number and M_r reflects the voids in the adsorbent. They are calculated and validated later in the result section. p_c is the controlling pressure of the condenser/evaporator, while p_e is the pressure in the reactor. Equation (11) calculates the equilibrium pressure of ammonia at different temperatures. R is the natural gas constant and ΔS is the entropy change according to the reactant.

$$\frac{dx}{dt} = Ar_a \cdot (1-x)^{Mr_a} \cdot \frac{p_c - p_{eq}}{p_c} \quad (9)$$

$$\frac{dx}{dt} = Ar_d \cdot x^{Mr_d} \cdot \frac{p_c - p_{eq}}{p_c} \quad (10)$$

$$p_{eq} = \exp\left(\frac{-\Delta H_r}{RT_c} + \frac{\Delta S}{R}\right) \quad (11)$$

2.4 Evaluation of the cogeneration system

The assessment of the cogeneration system includes the thermal efficiency in Equation (12). The indicator reflects the relationship between the output and input of the system.

$$\eta_{th} = \left(\dot{Q}_{ref} + \dot{W}_{net}\right) / [\dot{m}_h \cdot (h_{in} - h_{out})] \quad (12)$$

3. RESULTS AND DISCUSSION

3.1 Validation of kinetic models

The kinetic models of $MnCl_2$-ammonia adsorption and desorption phases are discovered and validated in Fig 2, using the experimental data from previous sorption performance tests. Table 1 lists the essential parameters.

	Adsorbent	Ar	Mr
Adsorption	$MnCl_2$-EG	0.009268	1.9
	$MnCl_2$-EG-Ni@C	0.013939	2.0
Desorption	$MnCl_2$-EG	5.9689×10^{-7}	1.115
	$MnCl_2$-EG-Ni@C	1.0319×10^{-6}	1.139

Table 1 Kinetic parameters of $MnCl_2$-EG

The global conversion ratios of four various experimental conditions are compared with the corresponding simulation results. The validation of desorption includes the 160 °C and 180 °C desorption, controlling the condenser at -20 °C, as shown in Fig 2 (a) and (c).

The computational results conform well to the experiments as the difference between the simulated and experimental ammonia conversion ratios is up to 0.049 in $MnCl_2$-EG, but in the results using novel sorbents, the error is larger by the desorption contraction. Moreover, the gap between the modelled and real data is relatively big with the value up to 0.09 in the validation of adsorption modelling. It is due to the reactive sorbents' appreciable expansion during adsorption. The agreement is still good between the simulations and the practical tests for the authors to use into the evaluation of the cogeneration systems.

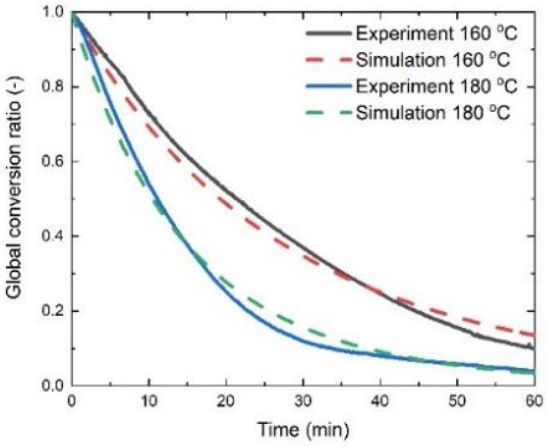

(a) Validation of $MnCl_2$-EG desorption kinetics

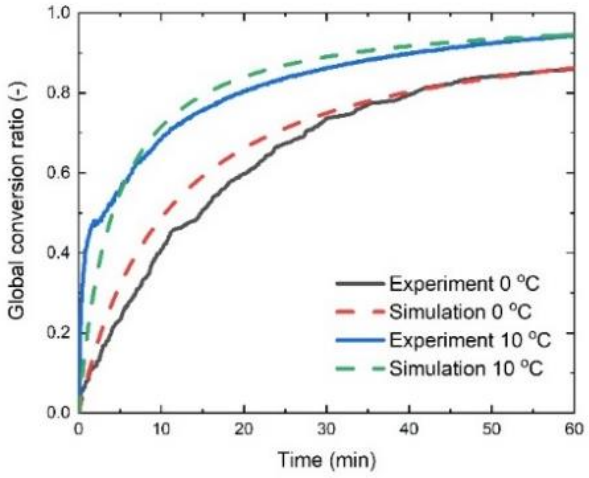

(b) Validation of $MnCl_2$-EG adsorption kinetics

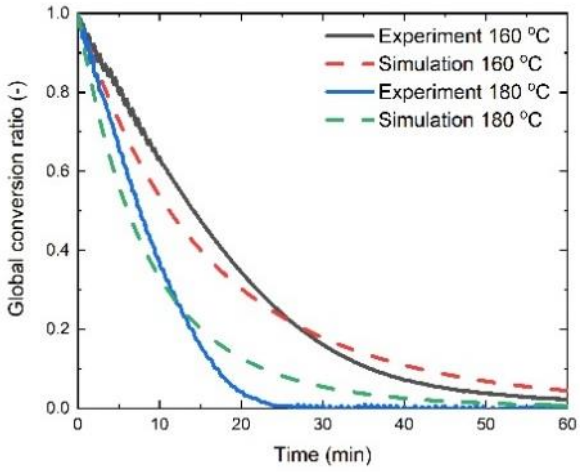

(c) Validation of $MnCl_2$-EG-Ni@C desorption kinetics

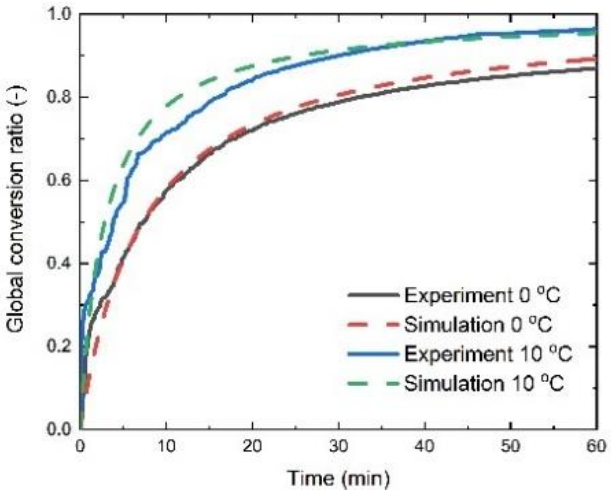

(d) Validation of $MnCl_2$-EG-Ni@C adsorption kinetics

Fig 2 Comparisons of experimental and simulated data

3.2 Simulation results

Fig 3 is the refrigeration generated by the integrated systems using the original sorbents of $MnCl_2$-EG or the novel one of $MnCl_2$-EG-Ni@C. The results

show AD-ORC has more cooling production than ORC-AD system, during the same reaction time. The reason is that using adsorption cycles as the first user of the heat source improves the desorption temperature of the sorbents. Thus, more ammonia is released in desorption process, resulting in the more active sorbent for next adsorption stage to absorb ammonia and produce cold effect. Setting the cycle time to 60 min, AD-ORC could enhance the cooling power to 2.16 times of that yielded by ORC-AD system.

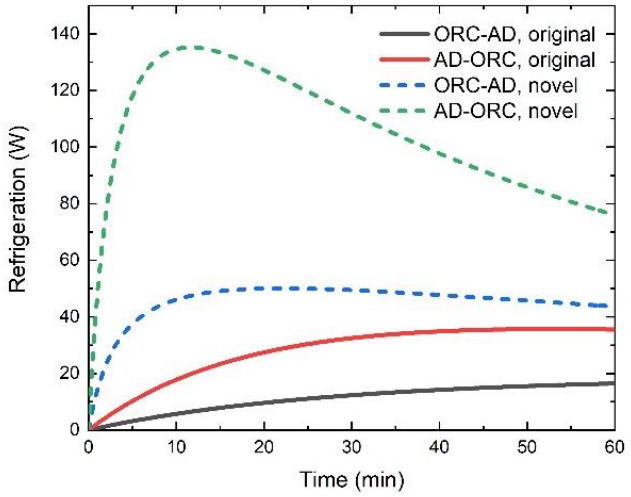

Fig 3 Refrigeration

Moreover, substituting the sorbent, refrigeration is improved in both systems, and the peak of the curve shows earlier than the original performance, demonstrating the accelerated reaction processes by using $MnCl_2$-EG-Ni@C. The highest refrigeration output is 135.21 W at 11.58 min, obtained from the simulation of AD-ORC system using $MnCl_2$-EG-Ni@C. At the end of 60 min, using novel sorbent could improve the refrigeration to 2.66 times or 2.14 times of the original ORC-AD or AD-ORC production, respectively.

Fig 4 illustrates the thermal efficiency of the low-grade heat recovery systems. The curves are in similar shapes of those in Fig 3. The phenomenon is caused by the definition equations of the thermal efficiency, when the power input and output of ORC are almost constant and the performance of sorption units plays significant roles in influencing the value of the system thermal efficiency. The results show the thermal efficiency of AD-ORC is lower than that of ORC-AD at the start, but it catches up with ORC-AD at 7.00 min. The explanation could be that, in the first seven minutes, the amount of the generated cooling power is not enough for dominating the thermal efficiency, while later the produced refrigeration could compete with the net power produced by ORC. Thus, the lack of net power caused by the moving of ORC position is filled by the refrigeration production after that time point. At the reaction time of 60 min, the improved thermal efficiency by moving the position of adsorption units is 0.3 % of the original value.

Besides, the short dash lines are higher than the solid lines, presenting the enhancement of the system thermal efficiencies by using $MnCl_2$-EG-Ni@C. In this condition, the highest thermal efficiency of ORC-AD is 6.91 % at 22.17 min, and that of AD-ORC is 7.04 % at 11.58 min. When the reaction time is 60 min, the combination with Ni@C could improve the thermal efficiency to 0.73 % and 1.02 % higher than that of ORC-AD and AD-ORC system, separately.

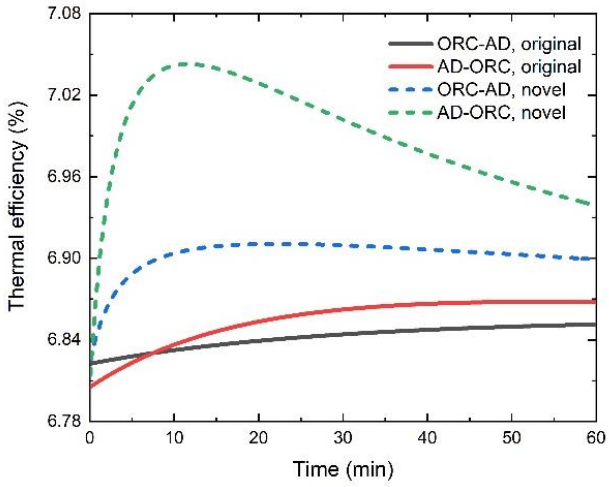

Fig 4 Thermal efficiency

Finally, it is worthy noting that the operational time is very crucial to the system performance. At the peak time of the short dash lines, the profit is the maximum. However, the feasibility of the time management needs more indicators to evaluate.

4. CONCLUSIONS

This paper establishes the kinetic models of $MnCl_2$-EG and $MnCl_2$-EG-Ni@C, based on the experimental data in previous explorations. Two cooling and power systems are built, integrating ORC with chemisorption technologies. The results present the validation of the sorption models with a satisfactory agreement.

Moreover, the refrigeration and the thermal efficiency is demonstrated to be higher in AD-ORC, compared with ORC-AD system. Using the sorbents with Ni@C could effectively enhance the refrigeration and the thermal efficiency.

ACKNOWLEDGEMENT

The authors would like to thank EPSRC for the support from the EPSRC Outcomes Award 2016 (EP/P511201/1) – Study of carbon-based Nanomaterials to enhance heat transfer and efficiency in chemisorption cogeneration system. The first author is grateful for the sponsorship towards her PhD projects from the Chinese Scholarship Council under No. 201608060039.

REFERENCE

[1] L. Talluri, D. Fiaschi, G. Neri, L. Ciappi, Design and optimization of a Tesla turbine for ORC applications, Applied Energy, 226 (2018) 300-319.

[2] S. Fujii, N. Horie, K. Nakaibayashi, Y. Kanematsu, Y. Kikuchi, T. Nakagaki, Design of zeolite boiler in thermochemical energy storage and transport system utilizing unused heat from sugar mill, Applied Energy, 238 (2019) 561-571.

[3] Y. Lu, Y. Wang, H. Bao, Et.al., Analysis of an optimal resorption cogeneration using mass and heat recovery processes, Applied Energy, 160 (2015) 892-901.

[4] Y. Lu, Y. Wang, C. Dong, Et.al., Design and assessment on a novel integrated system for power and refrigeration using waste heat from diesel engine, Applied Thermal Engineering, 91 (2015) 591-599.

[5] Y. Lu, A.P. Roskilly, K. Tang, Et.al., Investigation and performance study of a dual-source chemisorption power generation cycle using scroll expander, Applied Energy, 204 (2017) 979-993.

[6] F.N. Al-Mousawi, R. Al-Dadah, S. Mahmoud, Low grade heat driven adsorption system for cooling and power generation with small-scale radial inflow turbine, Applied Energy, 183 (2016) 1302-1316.

[7] H. Bao, Z. Ma, A.P. Roskilly, Chemisorption power generation driven by low grade heat – Theoretical analysis and comparison with pumpless ORC, Applied Energy, 186 (2017) 282-290.